Abstract

Background

Novel biological therapies have revolutionised the management of Rheumatoid Arthritis (RA) but no cure currently exists. Mesenchymal stem cells (MSCs) immunomodulate inflammatory responses through paracrine signalling via growth factors, cytokines, chemokines and extracellular vesicles (EVs) in the cell secretome; however, MSCs are still not available in the clinic. We evaluated the therapeutic potential of MSCs-derived EVs in an antigen-induced model of arthritis (AIA).

Methods

EVs isolated from MSCs in normal (21% O_2, 5% CO_2) or hypoxic (2% O_2, 5% CO_2) culture or from MSCs pre-conditioned with a pro-inflammatory cytokine cocktail were applied into the AIA model. Disease pathology was assessed 3 days post arthritis induction through histopathological analysis of knee joints. Spleens and lymph nodes were collected and assessed for T cell polarisation within the immune response to AIA. Activated naïve CD4+ T cells from spleens of healthy mice were cultured with EVs or MSCs to assess deactivation capabilities.

Results

All EV treatments significantly reduced knee-joint swelling and histopathological signs of AIA with enhanced responses to normoxic and pro-inflammatory primed EVs. Polarisation of T cells towards CD4+ helper cells expressing IL17a (Th17) was reduced when EV treatments from MSCs cultured in hypoxia or pro-inflammatory priming conditions were applied.

Conclusions

Hypoxically cultured EVs present a priming methodology that is as effective in reducing swelling, IL-17a expression, Th17 polarisation and T cell proliferation as pro-inflammatory priming. EVs present an effective novel technology for cell-free therapeutic translation in treating inflammatory arthritis and autoimmune disorders such as RA.

Background

Mesenchymal stem cells (MSCs) are a promising therapeutic option owing to their contribution to tissue repair, regeneration and immunomodulatory properties. As well as potential for tissue repair through trilineage differentiation capacity, MSCs influence immune responses through immunomodulation inhibiting T cell proliferation; disrupting B cell function and dendritic cell maturation; and promoting anti-inflammatory responses mediated through macrophage interactions(1). Widespread introduction of stem cell therapies has been hindered by the need to control and direct cell differentiation for tissue repair, particularly where tissue regeneration is not the primary goal of therapy as in the case of autoimmune disorders, such as Rheumatoid Arthritis (RA). For MSCs therapy, autologous bone marrow derived MSCs

are harvested and expanded to achieve therapeutic cell numbers, raising concerns over use of diseased donor cells and donor site morbidity due to invasive collection procedures, as well as potential variations that may occur during *in vitro* cell expansion.

Our group has demonstrated the immunomodulatory capacity of both MSCs and their conditioned medium (CM-MSC) to reduce inflammation in a murine antigen-induced arthritis (AIA) model(2, 3). MSCs function through several mechanisms: cell-to-cell contact, paracrine signalling and autocrine responses(1). CM-MSCs is rich in secreted paracrine signalling molecules and membrane bound vesicles that can target the cells of the immune system. Collection of CM-MSC harnesses MSCs expression of immunosuppressive factors which can be clinically applied in a therapeutic setting(4). Application of CM-MSC bypasses the need to introduce live cell therapy and therefore reduces the risk of inappropriate cell responses or unwanted tissue generation. CM-MSC is, however, not chemically defined owing to the complex cocktail of components secreted by cells during growth. The secretome of MSCs is high in signalling molecules, such as TGF-β1, IL-10, CCL9, IFN-α, IFN-β, nitric oxide (NO), VEGF, FGF, HGF, PDGF and membrane-bound vesicles(5). Extracellular vesicles (EVs) are lipid bilayer membrane bound particles that convey a cargo of nucleic acid, including microRNA (miRNA), long non-coding RNA, mRNA and DNA, lipid, carbohydrate and protein signals to facilitate intercellular communication(6–10). Notably, circulating EVs have been linked to disease severity in seropositive RA(11–16). These particles are typically < 1000 nm in diameter and can be subdivided by the mechanism of biogenesis. Exosomes are EVs synthesised in late endosomes, also known as multivesicular bodies (MVBs), and released through fusion of the MVBs with the plasma membrane, instead of being conveyed to the lysosome for catabolism(10). Microvesicles are EVs generated through outward budding and fission of the plasma membrane at locations enriched in specific lipids and proteins(5, 10). In contrast to viable cell infusions as therapy, EVs have no ability to replicate and their influence on gene regulation is through mRNA, non-coding RNAs and protein cargo(17). MSC-derived EVs have been shown to be beneficial in autoimmune disorders in functioning to modulate autoimmune responses, particularly related to graft rejection and hypertension(18–20) but also in inflammatory arthritis and rheumatic diseases(21–23). EVs are therefore of particular interest in autoimmune disorders and have been examined extensively in their ability to influence cells of the immune system (dendritic, B, T cells and macrophages)(13, 16, 24). Furthermore, secretion of EVs by immune cells can be induced through cell surface receptor activation and T cells have been shown to recruit EVs released by dendritic cells, suggesting an integral action in orchestrating *in vivo* immune responses(25, 26).

We previously demonstrated that the MSC secretome is responsible for the therapeutic effects of MSCs in an antigen-induced model of arthritis(3). Here we test our hypothesis that MSC-derived EVs alone can provide a valid alternative to MSC therapy overcoming major limitations which have prevented MSC therapy into the clinic. By delivering signalling biomolecules in a target-specific manner, EVs can influence cell responses in specific tissues dependent upon their surface molecule expression profile and can therefore be selected to directly influence specific cell types or tissues integral to the disease state. EVs can deliver their cargo into recipient cells through receptor-ligand interactions, direct fusion with the plasma membrane, antigen presentation and endocytosis (24, 25). The therapeutic potential of EVs may

be enhanced by manipulating their cargo to encourage therapeutic EVs to deliver a specific or targeted outcome, such as maximised anti-inflammatory capabilities(27, 28). The mechanisms by which cargo selection is achieved in EVs is becoming less opaque with greater clarity on the composition of MVBs and the interactions with the plasma membrane. Exosomes secreted by MVBs are sites for miRNA-loaded RNA-induced silencing complexes (RISCs) and microvesicle protein cargo is reflective of the plasma membranes of their generating cell type, suggesting that manipulation of the cell can directly lead to adaptive EV cargo(25, 29–33).

It is therefore important to clearly define the means by which EVs can be selected and a method to confirm positive identification. To standardise this process the International Society of Extracellular Vesicles (ISEV) has generated ongoing guidelines for minimal requirements to define isolated particles as EVs regardless of the selection methodology(34, 35). As the primary distinguishing feature of exosomes and microvesicles is their biogenesis, not their size, we will here refer to all isolated particles as EVs and eschew the terms exosome or microvesicle which remain contentious.

To date, no research has directly examined and contrasted the influence of cell isolation and priming on EVs generation using both hypoxia and pro-inflammatory pre-conditioning of MSCs during production. Here we apply these methods and contrast with cell therapy, to determine the variations in immunomodulatory properties, with a view to therapeutic application in autoimmune inflammatory disorders. We present novel data relevant to the therapeutic potential of MSC-derived EVs utilising the AIA model of inflammatory arthritis with direct comparison to the influence of their parental MSC through assessment of histological outcomes. We investigated the potential of primed MSCs using hypoxia and pro-inflammatory preconditioning to assess the optimisation of EV production through treatment of cells during EV production. The immunomodulatory action of primed MSC-derived EVs was investigated through examination of T cell activation, differentiation and proliferation, and quantification of immunomodulatory factors in comparison to EVs generated without MSC priming. We hypothesise that EVs represent a potential therapeutic approach for the treatment of inflammatory arthritis that may encounter less obstacles than cell therapy to widespread application in the clinic.

Methods

Cells and EVs

Primary human MSCs were isolated from commercially available bone marrow aspirate (Lonza, USA) using an adherence technique(36) and cultured in normoxic (21%O_2) or hypoxic (2%O_2) conditions in Dulbecco's Modified Eagles Medium (DMEM) with 10% foetal bovine serum (FBS) and 1% penicillin-streptomycin. Hypoxic cell culture was achieved using 2% O_2 from isolation of MSCs from bone marrow aspirate (Lonza) in hypoxic workstation (Invivo$_2$ Physiological Cell Culture Workstation, Baker Russkin) to ensure cells were not exposed to environmental oxygen levels at any stage of isolation or culture. Cells (P3-P5) were characterised as MSC through immunophenotyping of surface markers with flow cytometry and tri-lineage differentiation(2). EVs were therefore isolated over a 48 hour culture period from MSCs in

normoxic 21% oxygen culture (EV-NormO2); MSCs in hypoxic 2% oxygen culture (EV-2%O2) and from MSCs previously cultured for 48 hours with pro-inflammatory cytokine cocktail comprising interferon-gamma (IFN-γ, 10 ng/ml), tumour necrosis factor-alpha (TNFα, 10 ng/ml) and interleukin 1 beta (IL-1β, 5 ng/ml) prior to transfer to serum-free medium for 48 hours for EV collection (EV-Pro-Inflam).

Differential ultracentrifugation for isolation of EVs

MSCs from the same batch used for cell treatment (P3-P5) were cultured to 80–90% confluence in T75 flasks, washed with PBS three times and then serum-free DMEM. Flasks were incubated for 48 hours with 12 ml serum-free DMEM at 37 °C, 5% CO_2. After 48 hours, conditioned medium (CM-MSC) was removed and a cell count performed to determine the number of cells used to produce EVs. EVs were isolated from CM-MSC by differential ultracentrifugation. In brief, CM-MSC was centrifuged for 10 minutes at 300 *x g* to remove cell debris then again for 10 minutes at 2000 *x g* to remove apoptotic bodies and residual dead cells. Supernatant was again taken and centrifuged at 10,000 *x g* for 45 minutes in an ultracentrifuge (Beckman Coulter) to remove larger/denser EVs. Supernatant was again retrieved and passed through a 0.22 μM syringe filter. Filtered supernatant was then centrifuged using 70.1Ti rotor (Beckman Coulter) in a Beckman L8-55M ultracentrifuge at 100,000 *x g* for 90 minutes to isolate an EV pellet. EVs depleted medium was removed and stored at -20 °C (EVs-depleted CM-MSC), whilst the visible EVs pellet was resuspended in 5 ml of PBS to wash EVs and then spun again at 100,000 *x g* for 60 minutes, the supernatant discarded and the residual EV pellet resuspended in PBS at 30μL per 1.0×10^6 cells used in EV generation and stored at 4 °C to be used within 24 hours or at -20 °C for later use.

Characterisation of EVs

Successful isolation of EVs was confirmed through multiple methods in accordance with ISEV guidelines(35). Samples of vesicle preparations underwent bicinchoninic acid assay (BCA Assay, Pierce Biotechnology) for total protein concentration in EV preparations following manufacturer's instructions with EV disruption in a sonicating waterbath (30 seconds sonication at 1 minute intervals for 3 cycles) to release intracellular protein and assess cargo proteins as well as surface proteins. Vesicles were examined initially for expression of characteristic markers CD9, CD63 and CD81 (Miltenyi MACSPlex Exosome Identification Kit, human) following manufacturer's instructions for analysis. Particle by particle analysis of vesicle size was assessed using Nanopore technology (Izon Science) tuned in the region ~ 80–300 nm, to confirm the size fractions being applied experimentally.

Images of EVs were obtained using Transmission Electron Microscopy (TEM). EVs to be imaged by TEM were isolated as detailed above, however residual EV pellet after PBS wash was resuspended in 30 μl Milli-Q water per 3.0×10^6 cells. The resulting EV suspension was spotted onto a glow discharged holey carbon mesh copper grids (Quantifoil, R2/1) and incubated at room temperature for 4 min 45 seconds before 5μL of 0.22μ m filtered 2% (v/v) uranyl acetate was added. This was left to incubate at room temperature for a further 90 seconds before the excess liquid was removed using blotting paper. Grids were then imaged using an FEI Tecnai G2 12 Biotwin (LaB_6, accelerating voltage 100 kV).

EV protein content was examined by Western Blotting to identify the presence of Alix and absence of mitochondrial Cytochrome C (CYC1) in isolated particles, as per the minimal criteria for identification of EVs(34). Briefly, ten micrograms of EVs and cells were lysed with 2x Laemlli buffer with β-mercaptoethanol and denatured by heating at 70^{o}C for 5 min. Samples were electrophoresed on a 4–12% TGX stain free gel (Bio-Rad, CA, USA) at 200V for 30–40 min. Samples were then blotted onto a nitrocellulose membrane using the wet transfer method overnight at 100V. After blotting, membranes were blocked for 2 hours in 5% semi-skimmed milk in Tris-buffered saline with 0.05% Tween (TBST) followed by an incubation in primary antibodies Alix (1:200), CYC1 (1:200) (Santa Cruz Biotechnology, TX, US) for 2 hours at RT. After three five-minute washes, the membrane was probed with a goat anti-mouse IgG-HRP conjugated secondary antibody (1:1,000 in TBST, Life Technologies Limited, Paisley, UK). HRP-conjugated secondary antibody was added for 1 h and the wash step repeated. SuperSignal West Femto Chemiluminescent Substrate (Thermo Fisher Scientific, Waltham, MA, USA) was added to the membrane and imaged with ChemiDoc™ Touch Imaging System (Bio-Rad, CA, USA) using Image Lab v.6.0.1 software (Bio-Rad, CA, USA).

Antigen-induced arthritis (AIA) model of inflammatory arthritis

Animal procedures were undertaken in accordance with Home Office project licence PPL40/3594. AIA was induced in male C57Bl/6 mice (7–8 weeks) as previously described(2, 3, 37). Swelling was assessed by measuring the difference in diameter between the arthritic (right) and non-arthritic (left) knee joints (in mm) using a digital micrometer (Kroeplin GmbH) before and at set time points after treatment with PBS (control), EVs or EV-depleted CM-MSC.

Intra-articular injection of MSC and EVs

Treatments were 15 µl of EVs suspension corresponding to EV secretions from ~ 5.0×10^5 cells or EV-depleted CM-MSC (basal medium using serum free DMEM). Treatments or PBS vehicle control were injected intra-articularly 1 day post arthritis induction with 0.5 ml monoject (29G) insulin syringes (BD Micro-Fine, Franklyn Lakes, USA) through the patellar ligament into the right knee joint. Joint diameters were measured at 1, 2 and 3 days post injection. Blood, joints, spleen, inguinal and popliteal lymph nodes were collected immediately post-mortem. Three independent experiments were performed. All measures were taken to reduce animal numbers (n = 6–21 per condition).

Arthritis Index

Animals were sacrificed for histological analysis at day 3 post arthritis induction. Joints were fixed in 10% neutral buffered formal saline and decalcified in formic acid for 4 days at 4 °C before paraffin embedding. Sections (5 µm) were stained with haematoxylin and eosin (H&E) and mounted in Hydromount (National Diagnostics) as described previously(2, 3). H&E sections were scored for hyperplasia of the synovial intima (0 = normal to 3 = severe), cellular exudate (0 = normal to 3 = severe) and synovial infiltrate (0 = normal to 5 = severe) by two independent observers blinded to experimental groups(38). Scores were summated, producing a mean arthritis index.

Cytokine Quantification.

IL-10 and TNFα in serum and CM-MSC were quantified using mouse Quantikine ELISA IL-10 immunoassay (R&D Systems) and TNFα ELISA high sensitivity (eBioscience) respectively, following manufacturer's instructions.

T cell polarisation

Spleens and lymph nodes (popliteal/ inguinal) were collected from mice 3 days post-arthritis induction and dissociated as described previously(3). Splenocytes and pooled lymph node cells were seeded separately at 1.0×10^6 cells/well in 96-well plates (Sarstedt) in RPMI-1640 with 10% FBS, 0.05 µg/mL IL-2 and activated with cell stimulation cocktail (eBioscience) for 1 hour prior to adding 10 µg/ml brefeldin A (Sigma) and culturing for a further 4 hours. Unstimulated T cells and cells without brefeldin A served as negative controls. Following activation, cells were resuspended in 2 mM EDTA in PBS and Tregs (CD4 + CD25 + FOXP3+) were isolated using the CD4 + CD25 + Regulatory T Cell Isolation Kit (Miltenyi) following manufacturer's instructions; or stained for T cell subset identification. For this, cells were permeabilised using permeabilisation buffer kit (eBioscience) and intracellularly stained with anti-mouse IFN-γ (Th1), IL-4 (Th2) or IL17a (Th17) (eBioscience). Cells were analysed on a BD FACS Canto II flow cytometer and comparisons drawn for percentage CD4 + cells and signal intensity (XGeoMean) for each antibody.

Co-culture of T cells with MSC/CM-MSC

Proliferation of activated T cells was assessed as a measure of T cell deactivation. Initially, for positive controls 5×10^4 MSCs were cultured in 96-well plates for 24 hours at 37 °C. CD4 + T cells were purified from spleens and lymph nodes (popliteal/inguinal) of healthy C57Bl/6 mice using the CD4 + T Cell Isolation Kit (Miltenyi) following manufacturer's instructions. T cells were seeded at a density of 5.0×10^5/well in 250 µl RPMI medium with 10% FBS and cultured for 5 days with MSCs (ratio 10:1) or with EV-NormO2, EV-2%O2 or EV-Pro-Inflam (ratio equivalent to secretions from 10:1 cells) (n = 8). T cells alone served as control. Cells were activated using anti-Biotin MACSiBead Particles (Miltenyi) (ratio 2:1). EV treatments were refreshed after 2 days of culture. Polarisation was assessed as above and proliferation measured through reduction in signal intensity using VPD450 Violet proliferation dye (BD Biosciences) (3).

Statistical analysis

Data were tested for equal variance and normality using D'Agostino & Pearson omnibus normality test. Differences between groups were compared using 1-way ANOVA for parametric data or Kruskall-Wallis ANOVA for non-parametric, or 2-way ANOVA with Bonferroni correction, as stated. All statistical analysis was carried out using Prism 5 (GraphPad software) or IBM SPSS Statistics 24.0, with $P < 0.05$ deemed statistically significant. Results are expressed as mean ± confidence interval.

Results

EVs isolated via differential ultracentrifugation meet ISEV criteria

All EVs isolated in this study underwent a final 100,000 x g ultracentrifugation, a step that allows enrichment in small EVs. EV pellets were resuspended in a volume of PBS equivalent to 30 µl per 1.0 × 10^6 EV-secreting MSCs. Three distinct types of EV preparations were generated by culturing MSCs under normoxia (referred to as EV-NormO2; n = 11), hypoxia (referred to as EV-2%O2; n = 4) and pro-inflammatory conditions (referred to as EV-Pro-Inflam; n = 4), were used here as treatment both *in vitro* and *in vivo*.

A combination of quantitative and qualitative analyses were performed to confirm the presence of EVs and characterise their properties in EV-NormO2 preparations. Firstly, enrichment in characteristic exosome markers CD9, CD63 and CD81 in EV preparations from MSCs cultured under normoxic conditions was assessed by flow cytometry analysis using the MACSPlex exosome kit. This technology allows identification of 37 exosomal surface epitopes separated into individually identifiable populations using FITC and PE conjugation, then assessment of the percentage of epitope expression is achieved using APC conjugation for all epitopes within their individual populations. EV isolations showed elevated enrichment in CD9 (81.25 ± 5.03%), CD63 (94.59 ± 2.23%) and CD81 (79.41 ± 9.07%) (n = 11) (Fig. 1A) confirming the isolation of exosome enriched EVs. Secondly, western blot analysis of MSC lysate and EVs (EV-NormO2) for detection of Alix, a protein involved in MVB biogenesis, and cytochrome C, an ubiquitous mitochondrial protein acting as negative control, showed that isolated MSC-EVs are highly enriched in Alix, which is expressed by their cells of origin, but do not contain cytochrome C as expected (Fig. 1B). Thirdly, EVs were characterised for their size distribution and concentration using the Nanopore technology (Izon). EVs preparations showed a distribution of EV sizes with most prevalent diameter of ~ 200 nm with maximal diameter ~ 500 nm (Fig. 1D-E). Finally, TEM imaging demonstrated the presence of spherical vesicles in isolated preparations in accordance with ISEV criteria for single EVs characterisation (Fig. 1F). Together, these results demonstrate isolation of EVs meets ISEV criteria, confirming the presence of MSC-derived vesicles which can be confidently applied to our study.

MSC priming increases total protein content in EV cargo

Several cell priming approaches have been evaluated that enhance the anti-inflammatory, immunosuppressive, immunomodulatory, and regenerative properties of MSCs in order to increase their therapeutic efficacy. Here, we investigated the effect of MSC priming with hypoxia and inflammatory cytokines on EV secretion. As cell priming induces cell activation, molecular signalling, genetic or epigenetic modifications, and changes to cell morphology and phenotype, all of which involve changes in protein expression, we set out to determine whether the total protein content in the cargo of EVs was impacted by cell priming. A BCA assay revealed a trend for increased protein in EV-2%O2 preparations (81.29 ± 34.82 pg/1.0 × 10^6 cells; n = 8) and EV-Pro-inflam (69.09 ± 37.38 pg/1.0 × 10^6 cells; n = 9)

compared to EV-NormO2 (40.43 ± 14.73 pg/1.0 × 10^6 cells; n = 11) that was not statistically significant ($p > 0.05$) (Fig. 1C).

Application of MSC-derived EVs ameliorates histopathology and clinical symptoms of AIA

AIA is an acute model of inflammatory arthritis that typically exhibits peak joint swelling at 24 hours post induction with clinical symptoms and histopathological signs that resemble rheumatoid arthritis. Here, MSC-derived EV treatments were administered concurrent with peak joint swelling and joint diameter was measured daily up to day 3, and results were normalised to zero at day 1 peak joint swelling to minimise the impact of variations between animals. We have previously shown that the intra-articular injection of MSC conditioned medium in mice with AIA reduces joint swelling and histopathology (3). In this study, in order to assess the contribution of EVs to the therapeutic effect of the MSC secretome, we compared EV treatments to EV-depleted MSC conditioned medium, collected as described previously(3), and PBS only vehicle controls, measuring the reduction of joint diameter from peak swelling (day 1) as a positive value. Local administration of EVs into joints significantly reduced joint diameter, a measure of swelling. Specifically, EV-NormO2 (day 2 = 4.4 ± 0.6 mm, day 3 = 8.0 ± 0.6 mm, $p < 0.01$), EV-2%O2 (day 2 = 7.7 ± 0.8 mm, day 3 = 11.0 ± 0.9 mm, $p < 0.001$) and EV-Pro-inflam (day 2 = 6.7 ± 1.0 mm, day 3 = 11.3 ± 0.9 mm, $p < 0.001$) all very significantly reduce joint swelling in comparison to PBS vehicle control treatments (day 2 = 0.2 ± 0.8 mm, day 3 = 2.8 ± 1.0 mm) (Fig. 2A). Histopathological analysis of joint damage which is reported as arthritis index (AI) showed significantly reduced overall joint damage in mice treated with EV-NormO2 (4.20 ± 0.79) and EV-Pro-Inflam (4.08 ± 1.04) compared to EV-depleted medium control (7.46 ± 0.59). Whilst EV-2%O2 overall showed a tendency to reduce total AI scores (4.92 ± 0.84) compared to controls, this was not statistically significant. For EV-NormO2, this reduced AI score reflected decreases from control scores in hyperplasia of the synovial membrane (1.35 ± 0.22 vs 2.30 ± 0.17) and joint exudate (0.50 ± 0.21 vs 1.68 ± 0.30), whilst EV-Pro-Inflam demonstrated reduced synovial infiltrate (2.0 ± 0.39 vs 3.49 ± 0.24) (Fig. 2B).

Priming EVs does not affect expression of pro- (TNF-α) and anti-inflammatory (IL-10) cytokines detectable in serum of AIA mice

The pro-inflammatory cytokine TNF-α is a key driver of disease pathogenesis in RA and a therapeutic target in biological treatments(39, 40). Conversely, IL-10 is a master regulator of anti-inflammatory immune responses(7). Levels of TNF-α and IL-10 were measured at day 3 in the serum of mice following EV treatments. However, levels of TNF-α in serum of treated mice did not vary significantly between controls or treated conditions or between different treatment methodologies (Figure S1). ELISA on mouse serum did not detect the presence of IL-10 in treatment or control conditions (data not shown).

MSC-derived EVs reduce Th17 polarisation and restore the Th17:Treg balance

To examine the mechanism by which MSC-derived EVs significantly reduced AIA severity, spleens and lymph nodes (inguinal and popliteal) of EV-NormO2 and EV-depleted CM-MSC treated AIA mice and PBS controls were dissociated, and CD4 + T cells isolated. Overall, EV-NormO2 did not increase the proportion of CD4 + T cells in spleen (13.28 ± 0.51%) or lymph nodes (15.04 ± 1.04%) over PBS controls in spleen (14.21 ± 1.07%) or lymph nodes (15.52 ± 1.15%). However, EV-depleted CM-MSC treatment resulted in a statistically significant increase in CD4 + T cells in spleens (16.94 ± 0.81%, $p < 0.05$) compared to EV-NormO2 treatment, but not in lymph nodes (Fig. 3A, 3B).

Next, isolated, *in vivo* primed CD4 + T cells were activated and cultured *in vitro* for 4 hours in the presence of a membrane transport blocker. T cell polarisation was assessed by flow cytometry analysis of intracellular markers characteristic of Th1 (IFN-γ), Th2 (IL-4), Th17 (IL-17a) and regulatory T cells (CD25 + FOXP3+). In addition to the Th1/Th2 balance, the ratio of regulatory T cells (Tregs) to IL-17a expressing CD4 + T cells (Th17) was examined as RA (and other autoimmune disease) sufferers experience an imbalanced Th17:Treg ratio leading to inappropriate immune responses and tissue damage(41–44).

When compared to PBS control (3.23 ± 0.81%), spleen T cell polarisation towards Th17 effector cells following both EV-NormO2 (0.83 ± 0.10%) and EV-depleted CM-MSC (0.90 ± 0.19%) treatments showed significant decreases in the proportion of pro-inflammatory Th17 cells induced in AIA mice ($n = 4$, $p < 0.05$), with no significant change in FOXP3 (Treg) proportions (Fig. 3C, 3D). This translated to a trend for improved Treg:Th17 ratios in spleens of EV-NormO2 (12.06 ± 2.12:1) and EV-depleted CM-MSC (12.70 ± 2.95:1) treated mice compared to PBS controls (5.03 ± 1.40:1, $n = 4$, $p = 0.12$, $p = 0.09$ respectively) (Fig. 3E), despite an increase in pro-inflammatory Th1 cells in EV-NormO2 treated mice (6.38 ± 0.40%) compared to PBS controls (4.00 ± 0.35%, $p < 0.05$, $n = 4$) (Fig. 3F). This result indicates that EVs can prompt an advantageous shift in the Treg:Th17 balance towards a healthy state, demonstrating a similar efficacy of applying EVs alone to that previously seen when applying CM-MSC(3). A similar trend was seen in T cells from lymph nodes with a significant reduction in Th17 polarisation in EV (0.90 ± 0.09%) and EV-depleted CM-MSC (0.93 ± 0.25%) compared with PBS controls (4.26 ± 1.12%, $p < 0.05$, $n = 4$) (Fig. 3I) leading to improved Treg:Th17 ratio (Fig. 3J). Taken together, these data show that EV treatments and EV-depleted medium were both capable of affecting alleviation of symptoms of inflammatory arthritis through reduced Th17 polarisation and shift in the Treg:Th17 balance.

MSCs, not their EVs, enhance Th17 polarization when co-cultured with CD4 + T cells

MSCs have been shown to deactivate T cells in co-culture (2, 3). With this in mind, in order to further elucidate the influence of MSC-derived EV treatments on T cell polarisation and proliferation, EV-NormO2, EV-2%O2 and EV-Pro-Inflam were co-cultured with activated T cells isolated from healthy mice for 5 days.

Cells were then examined for changes in CD4 + cell numbers and Th17 polarization. The ability of EV treatments to affect deactivation of T cells and therefore influence T cell proliferation was also examined.

MSC/CD4 + T cell co-cultures prompted significantly increased numbers of CD4 + T cells compared to EV treatments or T cells alone ($n = 3$, $p < 0.05$) (Fig. 4A).

Further analysis of IL17a expressing cells within the CD4 + population demonstrated that MSC cultures increased cell proportions in comparison to PBS controls, whereas all EV treatments showed a decrease in Th17 cell polarisation ($p > 0.05$, $n = 3$) (Fig. 4B). IL-4 expressing Th2 cells were also elevated in MSC co-cultures (6.00 ± 0.24%) compared to EV-Pro-Inflam (2.74 ± 0.52%) ($p < 0.01$, $n = 3$) but not in comparison PBS control (4.79 ± 0.99%); EV-NormO2 (2.86 ± 0.30%) or EV-2%O2 (3.22 ± 0.03%) ($p > 0.05$, $n = 3$). Additionally, the expression of IL17a per cell, represented by mean fluorescence intensity (MFI) of signal, was significantly reduced in EV-NormO2 (3311.74 ± 33.71) and EV-2%O2/CD4 + T cell co-cultures (3367.19 ± 39.92) compared to CD4 + T cells cultured alone (3728.69 ± 50.28) ($p < 0.01$, $p < 0.05$, $n = 3$) (Fig. 4C). These results demonstrate that *in vitro* MSC-derived EVs do not prompt increases in CD4 + T cell numbers or Th17 effector cell polarisation as seen with MSC treatments, suggesting a further advantage in the therapeutic application of EVs over MSC.

MSCs, not their EVs, suppress T cell proliferation in co-culture

We have previously shown the ability of MSCs to suppress T cell proliferation in co-culture, with MSCs being more effective than CM-MSC(2, 3). Here, MSC/CD4 + T cell co-culture was included as a positive control and, similarly to our previous observations, it reduced the proportion of proliferating T cells, measured via a proliferative index and the number of proliferative cycles undergone by T cells in co-culture (5.31 ± 0.38, 4.63 ± 0.17 respectively) in comparison to T cells cultured alone (6.16 ± 0.10, 5.44 ± 0.25) ($n = 8$, $p < 0.05$). In contrast, CD4 + T cells showed no significant inhibition in proliferation when cultured with EV-NormO2 (5.85 ± 0.08, 5.01 ± 0.17), EV-2%O2 (6.01 ± 0.18, 4.97 ± 0.14) or EV-Pro-Inflam (6.28 ± 0.12, 4.95 ± 0.09) ($n = 8$, $p > 0.05$) (Fig. 4D). As seen previously with CM-MSC(3), EV treatments showed greater impact on proliferative cycles than on the proliferative index, though treatments did not significantly vary from either MSC co-cultures or T cells cultured alone, with the exception of pro-inflammatory primed EVs which allowed a higher proliferative index in comparison to MSC co-culture ($n = 8$, $p < 0.05$) (Fig. 4D). Together, this result, coupled with histological improvements, suggests that suppression of T cell proliferation may not be the key mechanism for improved outcomes following treatment in AIA.

Discussion

This study demonstrates the therapeutic efficacy of EVs as a treatment in the AIA model of inflammatory arthritis. All EV treatments prompted amelioration of clinical symptoms of AIA with increased effect seen in reduction of joint swelling when treated with EV-2%O2 or EV-Pro-Inflam. In line with this, histopathological examination of the joints showed improved histological features following EV

treatments compared to controls. Mechanistically, EVs acted remarkably different from their cells of origin (MSCs) when co-cultured with CD4 + T cells from healthy spleens. EVs reduced Th17 polarization without affecting T cell expansion and proliferation, while MSCs increased T cell expansion and Th17 polarization, and lessened T cell proliferation. *Ex vivo*, CD4 + T cells isolated from spleens of arthritic mice treated with EVs showed significantly reduced Th17 polarization that rebalanced the Treg:Th17 ratio. Together, this suggests the reduction in Th17 cells, that led to restoration of the Treg:Th17 ratio which is typically unbalanced in inflammatory arthritis, as the main therapeutic mode of action of MSC-derived EVs.

To further dissect the therapeutic mechanism of action of MSC-derived EVs, circulating levels of TNF-α, which is a key driver of pathogenesis in RA and therapeutic target in biological treatments, and IL-10, which is a master regulator of anti-inflammatory immune responses, were measured in mice with AIA at day 3. While IL-10 was not detected in our assay, similarly low levels of TNFa were detected in untreated and EV-treated mice. This suggests that TNFa blockade and IL-10 modulation are not the mechanisms by which MSC-derived EVs improve AIA and therefore EV treatment may represent an alternative option for patients who do not respond to biological interventions such as anti-TNF therapy. Nevertheless, a wider timecourse of serum TNF-α measurement (e.g. 14, 21 and 28 days) remains to be investigated.

Our previous study demonstrated reductions in Th17 cells following CM-MSC treatment compared to control and MSC treatments. It also showed an increase in IL-10 expression and proportions of IL-4 expressing Th2 cells as well as cellular expression levels of IL-4 following MSC treatment(3). We also demonstrated an improved Treg:Th17 effector cell ratio following CM-MSC treatment compared to MSC treatments or controls(3). With these results in mind, the present study indicates that MSCs, not their secretome, were driving increased IL-10 expression and were responsible for the reduction in Th1 and increase in Th2 cells seen in our previous study. Remarkably, EVs, a component of the CM-MSC, are capable of significantly reducing Th17 cell numbers. This represents a significant finding in the search for immunomodulatory therapeutics for treating autoimmune disorders where an imbalance in T cell polarisation (Th1:Th2 or Treg:Th17) is integral in disease pathology. Moreover, EV treatment in this study resulted in a highly improved (2.40-fold over controls) Treg:Th17 ratio compared to our previous results using whole CM-MSC treatment (2.13-fold over control) or MSC treatment (1.47-fold over control) (3).

The normal ratios of Treg:Th17 cells can be calculated from previously published studies by looking at proportions of either of these cell types in experimental investigations. The proportion of regulatory T cells in a healthy human is commonly reported in the range of 2.3–4.9 ± 1.1%(45–50), and the proportion of Th17 cells is reported at 0.50–2.13%(49–53) in peripheral blood, with typical murine Treg proportions reported at 10.2–12.1% in spleens(45, 47, 48, 54, 55) and Th17 cells at 1.17% in spleens(47, 56) respectively.

Therefore, using published research as above, a typical ratio of Treg:Th17 cells in healthy humans can be estimated to range from 1.1:1 to 9.8:1 and in healthy mice from 6.0:1 to 7.1:1.

In human RA sufferers the ratio of Treg:Th17 becomes imbalanced with peripheral blood Treg cells ranging from 1.0 to 16.9%(41, 53, 57) and Th17 cells ranging from 0.91 to 0.96%(42, 51) in peripheral blood, increasing to 2.20–9.09% in synovial fluid(42, 53). An analysis of published data from a range of studies shows that RA sufferers experience a drop in FOXP3 + Tregs from 5.94 ± 1.40% in healthy subjects to 4.44 ± 0.96% in patients, representing a 0.77 ± 0.07-fold decrease ($p = 0.021$, $n = 17$)(58). These data can be analysed to demonstrate a Treg:Th17 ratio ranging from 1.0:1 to 18.6:1 in peripheral blood and from 0.1:1 to 7.7:1 in synovial fluid of RA sufferers.

The proportions of Treg and Th17 cells in RA sufferers has been directly linked to the severity of disease, and restoring the Treg:Th17 balance has the potential to promote homeostasis and positive clinical outcomes by minimising inflammatory responses in a range of autoimmune disorders. Here, we demonstrate that untreated (control) spleens of mice with AIA display a Treg:Th17 ratio of 5:1 that is increased to 12:1 upon EV and EV-depleted CM-MSC treatments. This result reinforces the use of CM-MSC as a therapeutic for RA, with EVs being a convenient and chemically definable option for delivering its therapeutic action. Furthermore, the data in this study and our previous research suggest that CM-MSC might be a more effective therapeutic than MSCs for targeting inflammatory immune disorders such as RA, whilst MSCs might be more suitable for the treatment of inflammatory disorders, including Crohn's Disease, Lyme's arthritis, Multiple Sclerosis, Systemic Lupus Erythematosus, where tissue regeneration and the Th1/Th2 balance are an issue(59). The concomitant rise in IL-4 expressing Th2 cells and IL-10 in medium of MSC treatments but not CM-MSC seen previously would therefore be attributed to cellular interactions rather than secretome components.

Th17 and Treg differentiation are antagonistic responses to TGF-β expression, with low levels of TGF-β prompting synergy with IL6 and IL21 that in turn increases the expression of IL-23 receptor, resulting in upregulation of Th17 cell production. Conversely, highly expressed TGF-β prompts naïve helper T cells to express FOXP3 and retinoic acid receptor-related orphan receptor-γt (RORγt), and to repress the expression of IL-23 receptor, thus tilting the balance towards the generation of Treg cells where RORγt function is inhibited due to TGF-β induced FOXP3(60). Addition of IL-6, IL-21 and IL-23 restores RORγt function and associated Th17 differentiation(60–62). In this regard, our results demonstrate inhibition of IL17a production (or repressed IL-23 receptor expression) through EV treatment, inhibiting IL17a production whilst leaving the induction of FOXP3 expressing Treg cells unaffected.

Here, EV treatments did not induce IL-10 production, indicating that MSC-derived EV do not mediate anti-inflammatory effects via IL-10 as those seen in our previous study where MSCs and CM-MSC induced IL-10 release upon co-culture with T cells(3). IL-10 functions to inhibit monocyte-derived cell production of immunomodulatory cytokines such as IFN-γ and IL-4. This increases the likelihood that MSCs will convey a greater impact on Th1 and Th2 expressing cells than their secretome alone(7). Additionally, IL-10 expression prevents dendritic cell trafficking to lymph nodes, which presents a hypothesis for MSC action in reduced Th1 cell recruitment; however, here we demonstrate that lymph nodes show reductions only in IL17a expressing Th17 cells when treated with EVs, in accordance with the lack of IL-10 expression in medium previously shown (3).

In vivo, dendritic cell EVs which are high in expression of intercellular adhesion molecule 1 (ICAM-1) show high affinity binding to the surface of activated CD4 + T cells via the integrin leukocyte function-associated antigen 1 (LFA-1) without the need for T cell receptor specificity(26). This recruitment enables activated T cells to present acquired MHC class II peptide complexes from DCs and this can influence the activation and proliferation of the wider activated T cell population(63). MSCs are constitutively low in ICAM-1 expression(64, 65) however these cells have been shown to upregulate expression of ICAM-1 when co-cultured with activated CD4 + T cells in response to the presence of increased pro-inflammatory cytokine expression, leading to increased immunosuppressive properties of MSCs(64, 66). It follows then that priming MSCs with pro-inflammatory cytokines will enhance T cell adhesion to secreted EVs through increased binding efficiency and this has been shown to increase treatment potency(67, 68). It has been suggested that the immunomodulatory properties of EVs are contingent on pro-inflammatory priming(21, 69). However, the present work demonstrates that alternative priming methodologies, namely hypoxia, convey similarly enhanced immunosuppressive capabilities to secreted EVs.

Most studies utilise pro-inflammatory IFN-γ(70, 71) and/or TNF-α(72, 73) to facilitate priming, although IL-1β(74) and IL-17a(75) have also been applied. Regardless of cytokine selection, the broad outcomes of exposing cells in culture to a pro-inflammatory environment is to initiate strategies that would re-establish homeostatic control *in vivo*, such as anti-inflammatory effects prompted through alteration of the EV cargo(76) and signalling to reduce recruitment of inflammatory mediators, expression of pro-inflammatory cytokines, T cell polarisation and proliferation(71, 72, 77), and restoration of homeostatic ratios of leukocytes and T cells(73, 78). A primary mechanism involved here is IFN-γ-mediated upregulation of indoleamine 2,3-dioxygenase (IDO)(70, 72, 73).

Our study demonstrates that pro-inflammatory priming of MSCs does indeed increase the efficacy of EVs in treating inflammatory arthritis as observed in these studies. Our results suggest that the *in vivo* response to pro-inflammatory primed EV treatment in the AIA model of inflammatory arthritis is not primarily through inhibition of T cell proliferation, but through suppression of CD4 + Th17 effector polarisation.

However, we also show that hypoxic priming of MSCs results in the production of EVs that alleviate joint swelling as effectively as EVs secreted by MSCs primed with pro-inflammatory cytokines. This reduced swelling by EV-2%O2 treatment did not translate to significant improvement in the fine histological structures assessed in our arthritis index. Conversely, whilst both EV-2%O2 and EV-Pro-Inflam treatments inhibited polarisation of T cells towards pro-inflammatory Th17, EV-Pro-Inflam did not reduce the expression levels of IL-17a in Th17 cells as seen in EV-2%O2 treatments. We hypothesise that whilst the effectiveness of these treatment methodologies is similar in potency, the underlying mechanisms of action differ. Interestingly, MSCs under hypoxic culture have been shown to promote anti-inflammatory M2 macrophage polarization through a mechanism also dependent upon ICAM-1 adhesion(79), although hypoxic MSCs exhibit reduced reactive oxygen species (ROS) levels and increased resistance to ROS stress and upregulate secretion of growth factors and cytokines such as TGF-β, IL-8, IL-10 and PGE2, which are also implicated in macrophage polarisation and MSC immunomodulatory capacity(36, 79, 80).

Hypoxia inducible factor 1α (HIF-1α) is a primary sensor of hypoxia, and hypoxic conditions are physiologically common in regions of inflammation(81). Reduced oxygen environments are physiologically appropriate for MSCs resident in the bone marrow, where the available oxygen tensions are equivalent to 1–9% dependent upon distance from the vasculature, with the MSC niche likely to be resident in regions experiencing the lower end of this scale(36, 82). This makes EV-2%O2 a physiologically relevant treatment option derived from healthy conditions. We see primarily Th17 immunomodulation through EV treatment. The underlying mechanism by which EV-2%O2 treatment affects immunomodulation may be different to the mechanism(s) responsible for EV-Pro-Inflam-mediated effects, yet both hypoxic and pro-inflammatory cytokine priming systems may converge in affecting STAT3 activation. As described, RORγt is a master regulator of Th17 differentiation(60); however, STAT3 induces RORγt expression and is activated by IL-6, IL-21 and IL-23, which are key cytokines in promoting Th17 differentiation(60, 83). Moreover, STAT3 activation has been shown to be mandatory for the development of Th17 cells and Th17 related autoimmunity, such as seen in RA, and an absence of STAT3 activation inhibits Th17 formation and promotes Th1 differentiation through its absence, skewing pro-inflammatory immune responses from Th17 to Th1(83). STAT3 has been suggested as a therapeutic target in the treatment of autoimmune inflammatory disorders such as RA(81). In normoxic conditions the HIF-1 gene is inhibited by proteasome mediated degradation of HIF-1α and hydroxylation of HIF-1 by Factor Inhibiting HIF-1 protein (FIH)(84, 85). Hypoxia inhibits the function of key hydroxylases, von-Hippel-Lindau (VHL)-ubiquitin ligase complexes that mark HIF-1α protein for degradation in normoxia, and FIH. This in turn promotes increased HIF-1α protein in the cell due to reduced catabolism in degradative processes(84). Hif-1α dimerization with HIF-1β in the nucleus leads to transcriptional upregulation of genes in response to the hypoxia cues, primarily to drive metabolism from oxidative phosphorylation and oxygen-dependent ATP production towards glycolytic energy metabolism and decreased mitochondrial oxygen consumption. This reduces cellular dependency on oxygen, alongside activity that will restore oxygen supply to an affected region, such as angiogenesis achieved through regulation of target genes such as vascular endothelial growth factor (VEGF) and cathepsin D (CTSD)(81, 84, 85).

Priming of MSCs with hypoxia activates HIF-1α and increases cell signalling to induce these shifts in tissue energy metabolism and angiogenic responses to deal with the compromised inflammatory environment. It therefore follows that treatment with hypoxically induced changes to signalling molecules, such as EVs, conveys these coping mechanisms to the environment into which treatments are induced, promoting tissue stabilisation and homeostasis into the diseased joint cavity. These effects, in combination with enhanced immunomodulatory capacity due to increased TGF-β and IL-10 secretion and reduction in ROS due to hypoxic culture, led us to hypothesise that this mechanism of action may be more beneficial to cells. Prior exposure to pro-inflammatory cytokines prompt crisis responses in MSCs as evidenced through the induced cell death following continued exposure to pro-inflammatory cocktails we witnessed in our cell cultures if cytokine exposure exceeded 48 hours (data not shown).

Hypoxic culture of MSCs has been shown to aid maintenance of stemness and pluripotency in cells whilst very low oxygen tensions can assist in maintaining quiescence in resident stem cells, which may

be beneficial in clinical therapies dependent upon cell secretome rather than tissue regeneration(36). In this study, we observed a trend for increased protein content in hypoxic EV preparations compared to pro-inflammatory preconditioned cells, suggestive of a more potent EV treatment utilising this method of cell priming, which more closely mimic the physiological microenvironment. Previous studies have also demonstrated benefits of hypoxic treatment of MSCs and cell therapies for tissue repair in regenerative medicine treatments for arthritic disorders(86–93).

We have previously demonstrated CM-MSC reduced cartilage degradation by aggrecanase activity through ADAMTS and MMPs cleavage[3]. RA disease manifests with increased circulating citrullinated epitopes of degraded proteoglycans, including aggrecan, in > 60% of sufferers. This has implications in the production of pro-inflammatory cytokines directly linked to increased Th17 polarisation(41, 42, 58, 59). Circulating MHC-II complexes with cartilage epitope fragments may be implicated in the autoimmunity developed in RA through polarisation and activation of T cells, primarily Th17 effector cells(63). MMP activation occurs in response to pro-inflammatory signalling(63), and EVs sourced from stromal cells have been shown to carry both matrix metalloproteinases (MMPs), including MMP1, MMP2, MMP3, MMP7, MMP9 and MMP10, and ADAM9, ADAM10 and ADAMTS12(94, 95), and also tissue inhibitors of metalloproteinases (TIMPS) such as TIMP1, TIMP2 and TIMP3(94). Our previous study provided evidence of reduced activity of catabolic enzymes following CM-MSC treatment even beyond the effects seen with MSC infusion(3), thus the cargo of EVs may be the source of this mechanism of action in CM-MSC tests. EVs may function as a source of inhibitors of aggrecanases or equally introduce enzymes involved in epitope formation. As such, it would present an optimisation strategy to select EVs that carry a cargo high in TIMPs and anti-inflammatory cytokines, and low in aggrecanases. This presents a potential avenue for future investigation.

One common limitation in studies examining EVs is the presence of contaminating proteins present in EVs isolation through ultracentrifugation(24). Given the knowledge that both hypoxic and pro-inflammatory priming of MSCs can lead to increased expression of secreted proteins, it is important to ascertain whether the effects seen here could be the result of EVs contamination with proteins that also act to promote immunosuppression. In this study we utilised serum-free culture during EVs isolation to eliminate protein or EV contaminations from serum, and we included a PBS wash step during 100,000G ultracentrifugation to reduce residual protein. When measured, we saw no detectable IL-10 in T cell co-cultures suggesting an absence of IL-10 contamination in EVs preparations.

In this study, our primary aim was to evaluate the efficacy of EV treatments *in vivo* during AIA. We show that MSC priming leads to the release of EVs that if administered to mice with acute inflammatory arthritis significantly ameliorate disease pathogenesis, mainly by inhibiting Th17 polarization. Future studies will define the composition and sub-vesicular localisation of proteins in EV cargos.

Conclusions

This study provides new evidence that supports the use of EVs in clinical therapies for RA and similar autoimmune disorders. The possibility to manipulate the protein and nucleic acid cargo of EVs through control of parental MSC cultures offers a novel opportunity for targeted therapies that can be tailored to individual pathological features of RA, advancing personalised medicine. This study aims to support the growing body of evidence for the introduction of EVs into the therapeutic milieu. Further work on the control of EV cargo will elucidate the molecular mechanism of action and assist in the efficacy of cell-based therapies in the clinic.

Abbreviations

AIA – Antigen Induced Arthritis model

BCA – Bicinchoninic Acid Protein Assay

CM-MSC – MSCs derived conditioned medium

CTSD – Cathepsin D

CYC1 – Cytochrome C

DMEM – Dulbecco's Modified Eagle's Medium

EV-2%O2 – EVs derived from cells cultured in 2% oxygen

EV-NormO2 – EVs derived from cells cultured in normal environmental oxygen ~21%

EV-Pro-Inflam – EVs derived from MSCs cultured with pro-inflammatory cytokine stimulation

EVs – Extracellular vesicles

FBS – Foetal bovine serum

FIH – Factor inhibiting Hif-1 protein

H&E – Haematoxylin and eosin stain

HIF-1α – Hypoxia inducible factor 1 alpha

ICAM-1 – Intercellular adhesion molecule 1

IDO – Indoleamine 2,3-dioxygenase

IFN-γ – Interferon gamma

IL-10 – Interleukin 10

IL-1β – Interleukin 1 beta

ISEV – International Society of Extracellular Vesicles

LFA-1 – Leukocyte function associated antigen 1

MFI – Mean fluorescence intensity

miRNA – micro ribonucleic acid

MMPs – Matrix metalloproteins

MSCs – Mesenchymal stem/stromal cells

MVBs/MVEs – Multivesicular bodies/endosomes

NO – Nitric oxide

PBS – Phosphate buffered saline

RA – Rheumatoid Arthritis

RF – Rheumatoid factor

RISC – RNA-induced silencing complexes

RORγt – Retinoic acid receptor-related orphan receptor-γt

ROS – Reactive oxygen species

TIMPs – Tissue inhibitor of metalloproteinases

TNF-α – Tissue necrosis factor alpha

Treg – Regulatory T cell

VEGF – Vascular endothelial growth factor

VHL – von Hippel-Lindau ubiquitin ligase

Declarations

Ethics approval and consent to participate

All human cells were isolated from commercially sourced human bone marrow aspirate (Lonza). Animal procedures were undertaken in accordance with Home Office project licence PPL40/3594. All work was approved by the Keele University Research Ethics Committee.

Consent for publication

Not applicable

Availability of data and materials

Where possible, All data generated or analysed during this study are included in this published article [and its supplementary information files]. The datasets used and/or analysed during the current study are available from the corresponding author on reasonable request.

Competing Interests

The authors declare that they have no competing interests

Funding

This work was supported by the RJAH Orthopaedic Hospital Charity under Grant [G08028]; the UK EPSRC/MRC CDT in Regenerative Medicine (Keele University, Loughborough University, the University of Nottingham) under Grant [EP/F500491/1]; Orthopaedic Institute, Ltd under Grant [RPG 171].

Author's contributions

A.K. performed experimental work, wrote the manuscript and prepared all figures. K.T. provided support and technical skills for T cell investigations. P.R. gave technical expertise on Nanopore technology. R.M. provided support for histological investigations, TEM experiments and discussed and commented on the manuscript. R.L. performed TEM experiments. M.H. performed ELISAs and provided support for *in vivo* work and histological experiments. A.M.P. gave technical advice on data interpretations and presentation and reviewed the manuscript. N.R.F. contributed to experimental design. O.K. conceived and designed the research study, performed *in vivo* experiments, analysed data, wrote and supervised the manuscript. All authors reviewed the manuscript before submission.

Acknowledgements

The authors would like to thank the Nanoscale and Microscale Research Centre, University of Nottingham, for access to TEM facilities. We would like to thank Dr. Mark Platt (Loughborough University, UK) for his assistance in Nanopore technology.

References

1. Prockop DJ, Oh JY. Mesenchymal stem/stromal cells (MSCs): role as guardians of inflammation. Mol Ther. 2012;20(1):14-20.
2. Kehoe O, Cartwright A, Askari A, El Haj AJ, Middleton J. Intra-articular injection of mesenchymal stem cells leads to reduced inflammation and cartilage damage in murine antigen-induced arthritis. J Transl Med. 2014;12:157.

3. Kay AG, Long G, Tyler G, Stefan A, Broadfoot SJ, Piccinini AM, et al. Mesenchymal Stem Cell-Conditioned Medium Reduces Disease Severity and Immune Responses in Inflammatory Arthritis. Sci Rep. 2017;7(1):18019.
4. Grogan SP, Barbero A, Diaz-Romero J, Cleton-Jansen AM, Soeder S, Whiteside R, et al. Identification of markers to characterize and sort human articular chondrocytes with enhanced in vitro chondrogenic capacity. Arthritis Rheum. 2007;56(2):586-95.
5. Stanton H, Rogerson FM, East CJ, Golub SB, Lawlor KE, Meeker CT, et al. ADAMTS5 is the major aggrecanase in mouse cartilage in vivo and in vitro. Nature. 2005;434:648-52.
6. Beer KB, Rivas-Castillo J, Kuhn K, Fazeli G, Karmann B, Nance JF, et al. Extracellular vesicle budding is inhibited by redundant regulators of TAT-5 flippase localization and phospholipid asymmetry. Proc Natl Acad Sci U S A. 2018;115(6):E1127-E36.
7. Couper KN, Blount DG, Riley EM. IL-10: the master regulator of immunity to infection. J Immunol. 2008;180(9):5771-7.
8. Kusuma GD, Barabadi M, Tan JL, Morton DAV, Frith JE, Lim R. To Protect and to Preserve: Novel Preservation Strategies for Extracellular Vesicles. Front Pharmacol. 2018;9:1199.
9. Muralidharan-Chari V, Clancy JW, Sedgwick A, D'Souza-Schorey C. Microvesicles: mediators of extracellular communication during cancer progression. J Cell Sci. 2010;123(Pt 10):1603-11.
10. Raposo G, Stoorvogel W. Extracellular vesicles: exosomes, microvesicles, and friends. J Cell Biol. 2013;200(4):373-83.
11. Burbano C, Rojas M, Munoz-Vahos C, Vanegas-Garcia A, Correa LA, Vasquez G, et al. Extracellular vesicles are associated with the systemic inflammation of patients with seropositive rheumatoid arthritis. Sci Rep. 2018;8(1):17917.
12. Arntz OJ, Pieters BCH, Thurlings RM, Wenink MH, van Lent P, Koenders MI, et al. Rheumatoid Arthritis Patients With Circulating Extracellular Vesicles Positive for IgM Rheumatoid Factor Have Higher Disease Activity. Front Immunol. 2018;9:2388.
13. Messer L, Alsaleh G, Freyssinet JM, Zobairi F, Leray I, Gottenberg JE, et al. Microparticle-induced release of B-lymphocyte regulators by rheumatoid synoviocytes. Arthritis Res Ther. 2009;11(2):R40.
14. Lo Cicero A, Majkowska I, Nagase H, Di Liegro I, Troeberg L. Microvesicles shed by oligodendroglioma cells and rheumatoid synovial fibroblasts contain aggrecanase activity. Matrix Biol. 2012;31(4):229-33.
15. Zhang HG, Liu C, Su K, Yu S, Zhang L, Zhang S, et al. A membrane form of TNF-alpha presented by exosomes delays T cell activation-induced cell death. J Immunol. 2006;176(12):7385-93.
16. Kim SH, Lechman ER, Bianco N, Menon R, Keravala A, Nash J, et al. Exosomes derived from IL-10-treated dendritic cells can suppress inflammation and collagen-induced arthritis. J Immunol. 2005;174(10):6440-8.
17. Balaj L, Lessard R, Dai L, Cho YJ, Pomeroy SL, Breakefield XO, et al. Tumour microvesicles contain retrotransposon elements and amplified oncogene sequences. Nat Commun. 2011;2:180.

18. Lee C, Mitsialis SA, Aslam M, Vitali SH, Vergadi E, Konstantinou G, et al. Exosomes mediate the cytoprotective action of mesenchymal stromal cells on hypoxia-induced pulmonary hypertension. Circulation. 2012;126(22):2601-11.
19. Mokarizadeh A, Delirezh N, Morshedi A, Mosayebi G, Farshid AA, Mardani K. Microvesicles derived from mesenchymal stem cells: potent organelles for induction of tolerogenic signaling. Immunol Lett. 2012;147(1-2):47-54.
20. Zhang B, Yin Y, Lai RC, Tan SS, Choo AB, Lim SK. Mesenchymal stem cells secrete immunologically active exosomes. Stem Cells Dev. 2014;23(11):1233-44.
21. Cosenza S, Toupet K, Maumus M, Luz-Crawford P, Blanc-Brude O, Jorgensen C, et al. Mesenchymal stem cells-derived exosomes are more immunosuppressive than microparticles in inflammatory arthritis. Theranostics. 2018;8(5):1399-410.
22. Alcaraz MJ, Compan A, Guillen MI. Extracellular Vesicles from Mesenchymal Stem Cells as Novel Treatments for Musculoskeletal Diseases. Cells. 2019;9(1).
23. Ma D, Xu K, Zhang G, Liu Y, Gao J, Tian M, et al. Immunomodulatory effect of human umbilical cord mesenchymal stem cells on T lymphocytes in rheumatoid arthritis. Int Immunopharmacol. 2019;74:105687.
24. Gyorgy B, Szabo TG, Pasztoi M, Pal Z, Misjak P, Aradi B, et al. Membrane vesicles, current state-of-the-art: emerging role of extracellular vesicles. Cell Mol Life Sci. 2011;68(16):2667-88.
25. Thery C, Ostrowski M, Segura E. Membrane vesicles as conveyors of immune responses. Nat Rev Immunol. 2009;9(8):581-93.
26. Nolte-'t Hoen EN, Buschow SI, Anderton SM, Stoorvogel W, Wauben MH. Activated T cells recruit exosomes secreted by dendritic cells via LFA-1. Blood. 2009;113(9):1977-81.
27. Lo Sicco C, Reverberi D, Balbi C, Ulivi V, Principi E, Pascucci L, et al. Mesenchymal Stem Cell-Derived Extracellular Vesicles as Mediators of Anti-Inflammatory Effects: Endorsement of Macrophage Polarization. Stem Cells Transl Med. 2017;6(3):1018-28.
28. Di Trapani M, Bassi G, Midolo M, Gatti A, Kamga PT, Cassaro A, et al. Differential and transferable modulatory effects of mesenchymal stromal cell-derived extracellular vesicles on T, B and NK cell functions. Sci Rep. 2016;6:24120.
29. Gibbings DJ, Ciaudo C, Erhardt M, Voinnet O. Multivesicular bodies associate with components of miRNA effector complexes and modulate miRNA activity. Nat Cell Biol. 2009;11(9):1143-9.
30. Géminard C, de Gassart A, Blanc L, Vidal M. Degradation of AP2 During Reticulocyte Maturation Enhances Binding of Hsc70 and Alix to a Common Site on TfR for Sorting into Exosomes. Traffic. 2004;5:181-93.
31. Buschow SI, Nolte-'t Hoen ENM, van Niel G, Pols MS, ten Broeke T, Lauwen M, et al. MHC II in Dendritic Cells is Targeted to Lysosomes or T Cell-Induced Exosomes Via Distinct Multivesicular Body Pathways. Traffic. 2009;10(10):1528-42.
32. Nabhan JF, Hu R, Oh RS, Cohen SN, Lu Q. Formation and release of arrestin domain-containing protein 1-mediated microvesicles (ARMMs) at plasma membrane by recruitment of TSG101 protein.

Proc Natl Acad Sci U S A. 2012;109(11):4146-51.

33. Shen B, Fang Y, Wu N, Gould SJ. Biogenesis of the posterior pole is mediated by the exosome/microvesicle protein-sorting pathway. J Biol Chem. 2011;286(51):44162-76.
34. Lotvall J, Hill AF, Hochberg F, Buzas EI, Di Vizio D, Gardiner C, et al. Minimal experimental requirements for definition of extracellular vesicles and their functions: a position statement from the International Society for Extracellular Vesicles. J Extracell Vesicles. 2014;3:26913.
35. Thery C, Witwer KW, Aikawa E, Alcaraz MJ, Anderson JD, Andriantsitohaina R, et al. Minimal information for studies of extracellular vesicles 2018 (MISEV2018): a position statement of the International Society for Extracellular Vesicles and update of the MISEV2014 guidelines. J Extracell Vesicles. 2018;7(1):1535750.
36. Kay AG, Dale TP, Akram KM, Mohan P, Hampson K, Maffulli N, et al. BMP2 repression and optimized culture conditions promote human bone marrow-derived mesenchymal stem cell isolation. Regen Med. 2015;10(2):109-25.
37. Glant TT, Ocsko T, Markovics A, Szekanecz Z, Katz RS, Rauch TA, et al. Characterization and Localization of Citrullinated Proteoglycan Aggrecan in Human Articular Cartilage. PLoS One. 2016;11(3):e0150784.
38. Misjak P, Bosze S, Horvati K, Pasztoi M, Paloczi K, Holub MC, et al. The role of citrullination of an immunodominant proteoglycan (PG) aggrecan T cell epitope in BALB/c mice with PG-induced arthritis. Immunol Lett. 2013;152(1):25-31.
39. Djouad F, Fritz V, Apparailly F, Louis-Plence P, Bony C, Sany J, et al. Reversal of the immunosuppressive properties of mesenchymal stem cells by tumor necrosis factor alpha in collagen-induced arthritis. Arthritis Rheum. 2005;52(5):1595-603.
40. Firestein GS. Rheumatoid arthritis in a mouse? Nat Clin Pract Rheumatol. 2009;5(1):1.
41. Al-Zifzaf DS, El Bakry SA, Mamdouh R, Shawarby LA, Ghaffar AYA, Amer HA, et al. FoxP3+T regulatory cells in Rheumatoid arthritis and the imbalance of the Treg/TH17 cytokine axis. The Egyptian Rheumatologist. 2015;37(1):7-15.
42. Arroyo-Villa I, Bautista-Caro MB, Balsa A, Aguado-Acin P, Nuno L, Bonilla-Hernan MG, et al. Frequency of Th17 CD4+ T cells in early rheumatoid arthritis: a marker of anti-CCP seropositivity. PLoS One. 2012;7(8):e42189.
43. Diller ML, Kudchadkar RR, Delman KA, Lawson DH, Ford ML. Balancing Inflammation: The Link between Th17 and Regulatory T Cells. Mediators of Inflammation. 2016;2016:1-8.
44. Noack M, Miossec P. Th17 and regulatory T cell balance in autoimmune and inflammatory diseases. Autoimmun Rev. 2014;13(6):668-77.
45. Rodriguez-Perea AL, Arcia ED, Rueda CM, Velilla PA. Phenotypical characterization of regulatory T cells in humans and rodents. Clin Exp Immunol. 2016;185(3):281-91.
46. Rodriguez-Perea AL, Montoya CJ, Olek S, Chougnet CA, Velilla PA. Statins increase the frequency of circulating CD4+ FOXP3+ regulatory T cells in healthy individuals. J Immunol Res. 2015;2015:762506.

47. Schmitt EG, Williams CB. Generation and function of induced regulatory T cells. Front Immunol. 2013;4:152.
48. Dias S, D'Amico A, Cretney E, Liao Y, Tellier J, Bruggeman C, et al. Effector Regulatory T Cell Differentiation and Immune Homeostasis Depend on the Transcription Factor Myb. Immunity. 2017;46(1):78-91.
49. Li L, Yang C, Zhao Z, Xu B, Zheng M, Zhang C, et al. Skewed T-helper (Th)1/2- and Th17/T regulatorycell balances in patients with renal cell carcinoma. Mol Med Rep. 2015;11(2):947-53.
50. Li S, Li Y, Qu X, Liu X, Liang J. Detection and significance of TregFoxP3(+) and Th17 cells in peripheral blood of non-small cell lung cancer patients. Arch Med Sci. 2014;10(2):232-9.
51. Shen H, Goodall JC, Hill Gaston JS. Frequency and phenotype of peripheral blood Th17 cells in ankylosing spondylitis and rheumatoid arthritis. Arthritis Rheum. 2009;60(6):1647-56.
52. Chen H, Ren X, Liao N, Wen F. Th17 cell frequency and IL-17A concentrations in peripheral blood mononuclear cells and vitreous fluid from patients with diabetic retinopathy. J Int Med Res. 2016;44(6):1403-13.
53. Nistala K, Moncrieffe H, Newton KR, Varsani H, Hunter P, Wedderburn LR. Interleukin-17-producing T cells are enriched in the joints of children with arthritis, but have a reciprocal relationship to regulatory T cell numbers. Arthritis Rheum. 2008;58(3):875-87.
54. Curotto de Lafaille MA, Lino AC, Kutchukhidze N, Lafaille JJ. CD25- T cells generate CD25+Foxp3+ regulatory T cells by peripheral expansion. J Immunol. 2004;173(12):7259-68.
55. Kretschmer K, Apostolou I, Hawiger D, Khazaie K, Nussenzweig MC, von Boehmer H. Inducing and expanding regulatory T cell populations by foreign antigen. Nat Immunol. 2005;6(12):1219-27.
56. Li K, Wang Z, Cao Y, Bunjhoo H, Zhu J, Chen Y, et al. The study of the ratio and distribution of Th17 cells and Tc17 cells in asthmatic patients and the mouse model. Asian Pac J Allergy Immunol. 2013;31(2):125-31.
57. Cribbs AP, Kennedy A, Penn H, Read JE, Amjadi P, Green P, et al. Treg cell function in rheumatoid arthritis is compromised by ctla-4 promoter methylation resulting in a failure to activate the indoleamine 2,3-dioxygenase pathway. Arthritis Rheumatol. 2014;66(9):2344-54.
58. Morita T, Shima Y, Wing JB, Sakaguchi S, Ogata A, Kumanogoh A. The Proportion of Regulatory T Cells in Patients with Rheumatoid Arthritis: A Meta-Analysis. PLoS One. 2016;11(9):e0162306.
59. D'Elios M, Del Prete G. Th1/Th2 Balance in human disease. Transplant Proc. 1998;30:2373-7.
60. Zhou L, Lopes JE, Chong MM, Ivanov, II, Min R, Victora GD, et al. TGF-beta-induced Foxp3 inhibits T(H)17 cell differentiation by antagonizing RORgammat function. Nature. 2008;453(7192):236-40.
61. Zhou L, Ivanov, II, Spolski R, Min R, Shenderov K, Egawa T, et al. IL-6 programs T(H)-17 cell differentiation by promoting sequential engagement of the IL-21 and IL-23 pathways. Nat Immunol. 2007;8(9):967-74.
62. Korn T, Bettelli E, Gao W, Awasthi A, Jager A, Strom TB, et al. IL-21 initiates an alternative pathway to induce proinflammatory T(H)17 cells. Nature. 2007;448(7152):484-7.

63. Helft J, Jacquet A, Joncker NT, Grandjean I, Dorothee G, Kissenpfennig A, et al. Antigen-specific T-T interactions regulate CD4 T-cell expansion. Blood. 2008;112(4):1249-58.
64. Ren G, Zhao X, Zhang L, Zhang J, L'Huillier A, Ling W, et al. Inflammatory cytokine-induced intercellular adhesion molecule-1 and vascular cell adhesion molecule-1 in mesenchymal stem cells are critical for immunosuppression. J Immunol. 2010;184(5):2321-8.
65. Shi Y, Su J, Roberts AI, Shou P, Rabson AB, Ren G. How mesenchymal stem cells interact with tissue immune responses. Trends Immunol. 2012;33(3):136-43.
66. Ren G, Zhang L, Zhao X, Xu G, Zhang Y, Roberts AI, et al. Mesenchymal stem cell-mediated immunosuppression occurs via concerted action of chemokines and nitric oxide. Cell Stem Cell. 2008;2(2):141-50.
67. Kavanagh DP, Robinson J, Kalia N. Mesenchymal stem cell priming: fine-tuning adhesion and function. Stem Cell Rev Rep. 2014;10(4):587-99.
68. Djouad F, Plence P, Bony C, Tropel P, Apparailly F, Sany J, et al. Immunosuppressive effect of mesenchymal stem cells favors tumor growth in allogeneic animals. Blood. 2003;102(10):3837-44.
69. Maumus M, Roussignol G, Toupet K, Penarier G, Bentz I, Teixeira S, et al. Utility of a Mouse Model of Osteoarthritis to Demonstrate Cartilage Protection by IFNgamma-Primed Equine Mesenchymal Stem Cells. Front Immunol. 2016;7:392.
70. Chinnadurai R, Copland IB, Patel SR, Galipeau J. IDO-independent suppression of T cell effector function by IFN-gamma-licensed human mesenchymal stromal cells. J Immunol. 2014;192(4):1491-501.
71. Chinnadurai R, Rajan D, Ng S, McCullough K, Arafat D, Waller EK, et al. Immune dysfunctionality of replicative senescent mesenchymal stromal cells is corrected by IFNgamma priming. Blood Adv. 2017;1(11):628-43.
72. Francois M, Romieu-Mourez R, Li M, Galipeau J. Human MSC suppression correlates with cytokine induction of indoleamine 2,3-dioxygenase and bystander M2 macrophage differentiation. Mol Ther. 2012;20(1):187-95.
73. Rovira Gonzalez YI, Lynch PJ, Thompson EE, Stultz BG, Hursh DA. In vitro cytokine licensing induces persistent permissive chromatin at the Indoleamine 2,3-dioxygenase promoter. Cytotherapy. 2016;18(9):1114-28.
74. Carrero R, Cerrada I, Lledo E, Dopazo J, Garcia-Garcia F, Rubio MP, et al. IL1beta induces mesenchymal stem cells migration and leucocyte chemotaxis through NF-kappaB. Stem Cell Rev Rep. 2012;8(3):905-16.
75. Sivanathan KN, Rojas-Canales DM, Hope CM, Krishnan R, Carroll RP, Gronthos S, et al. Interleukin-17A-Induced Human Mesenchymal Stem Cells Are Superior Modulators of Immunological Function. Stem Cells. 2015;33(9):2850-63.
76. Hyland M, Mennan C, Wilson E, Clayton A, Kehoe O. Pro-Inflammatory Priming of Umbilical Cord Mesenchymal Stromal Cells Alters the Protein Cargo of Their Extracellular Vesicles. Cells. 2020;9(3).

77. Monguio-Tortajada M, Roura S, Galvez-Monton C, Pujal JM, Aran G, Sanjurjo L, et al. Nanosized UCMSC-derived extracellular vesicles but not conditioned medium exclusively inhibit the inflammatory response of stimulated T cells: implications for nanomedicine. Theranostics. 2017;7(2):270-84.
78. Noronha NC, Mizukami A, Caliari-Oliveira C, Cominal JG, Rocha JLM, Covas DT, et al. Priming approaches to improve the efficacy of mesenchymal stromal cell-based therapies. Stem Cell Res Ther. 2019;10(1):131.
79. Takizawa N, Okubo N, Kamo M, Chosa N, Mikami T, Suzuki K, et al. Bone marrow-derived mesenchymal stem cells propagate immunosuppressive/anti-inflammatory macrophages in cell-to-cell contact-independent and -dependent manners under hypoxic culture. Exp Cell Res. 2017;358(2):411-20.
80. Li B, Li C, Zhu M, Zhang Y, Du J, Xu Y, et al. Hypoxia-Induced Mesenchymal Stromal Cells Exhibit an Enhanced Therapeutic Effect on Radiation-Induced Lung Injury in Mice due to an Increased Proliferation Potential and Enhanced Antioxidant Ability. Cell Physiol Biochem. 2017;44(4):1295-310.
81. Gaffen SL, Jain R, Garg AV, Cua DJ. The IL-23-IL-17 immune axis: from mechanisms to therapeutic testing. Nat Rev Immunol. 2014;14(9):585-600.
82. Mohyeldin A, Garzon-Muvdi T, Quinones-Hinojosa A. Oxygen in stem cell biology: a critical component of the stem cell niche. Cell Stem Cell. 2010;7(2):150-61.
83. Harris TJ, Grosso JF, Yen HR, Xin H, Kortylewski M, Albesiano E, et al. Cutting edge: An in vivo requirement for STAT3 signaling in TH17 development and TH17-dependent autoimmunity. J Immunol. 2007;179(7):4313-7.
84. Dengler VL, Galbraith M, Espinosa JM. Transcriptional regulation by hypoxia inducible factors. Crit Rev Biochem Mol Biol. 2014;49(1):1-15.
85. Dang EV, Barbi J, Yang HY, Jinasena D, Yu H, Zheng Y, et al. Control of T(H)17/T(reg) balance by hypoxia-inducible factor 1. Cell. 2011;146(5):772-84.
86. Adesida AB, Mulet-Sierra A, Jomha NM. Hypoxia mediated isolation and expansion enhances the chondrogenic capacity of bone marrow mesenchymal stromal cells. Stem Cell Res Ther. 2012;3(2):9.
87. Baumgartner L, Arnhold S, Brixius K, Addicks K, Bloch W. Human mesenchymal stem cells: Influence of oxygen pressure on proliferation and chondrogenic differentiation in fibrin glue in vitro. J Biomed Mater Res A. 2010;93(3):930-40.
88. Farrell MJ, Shin JI, Smith LJ, Mauck RL. Functional consequences of glucose and oxygen deprivation on engineered mesenchymal stem cell-based cartilage constructs. Osteoarthritis Cartilage. 2015;23(1):134-42.
89. Fehrer C, Brunauer R, Laschober G, Unterluggauer H, Reitinger S, Kloss F, et al. Reduced oxygen tension attenuates differentiation capacity of human mesenchymal stem cells and prolongs their lifespan. Aging Cell. 2007;6(6):745-57.
90. Felka T, Schafer R, Schewe B, Benz K, Aicher WK. Hypoxia reduces the inhibitory effect of IL-1beta on chondrogenic differentiation of FCS-free expanded MSC. Osteoarthritis Cartilage. 2009;17(10):1368-

76.

91. Gawlitta D, van Rijen MH, Schrijver EJ, Alblas J, Dhert WJ. Hypoxia impedes hypertrophic chondrogenesis of human multipotent stromal cells. Tissue Eng Part A. 2012;18(19-20):1957-66.
92. Grayson WL, Zhao F, Bunnell B, Ma T. Hypoxia enhances proliferation and tissue formation of human mesenchymal stem cells. Biochem Biophys Res Commun. 2007;358(3):948-53.
93. Kay A, Richardson J, Forsyth NR. Physiological normoxia and chondrogenic potential of chondrocytes. Front Biosci (Elite Ed). 2011;3(1945-0508 (Electronic)):1365-74.
94. Lai RC, Tan SS, Teh BJ, Sze SK, Arslan F, de Kleijn DP, et al. Proteolytic Potential of the MSC Exosome Proteome: Implications for an Exosome-Mediated Delivery of Therapeutic Proteasome. Int J Proteomics. 2012;2012:971907.
95. Shimoda M, Khokha R. Proteolytic factors in exosomes. Proteomics. 2013;13(10-11):1624-36.

Figures

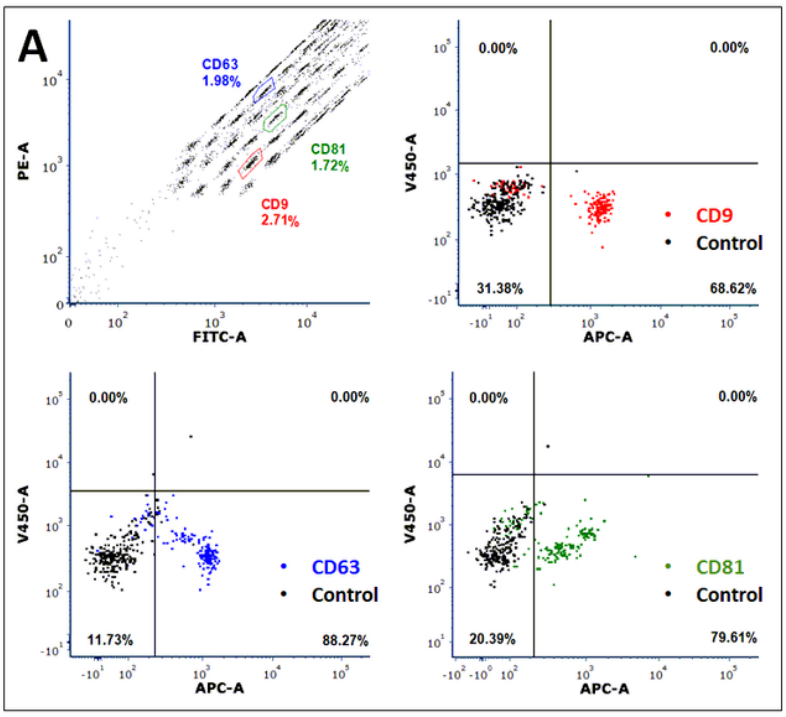

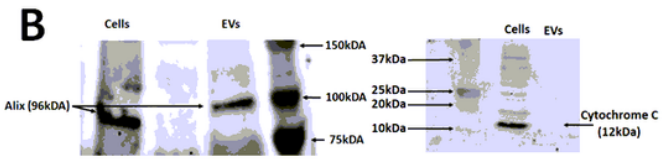

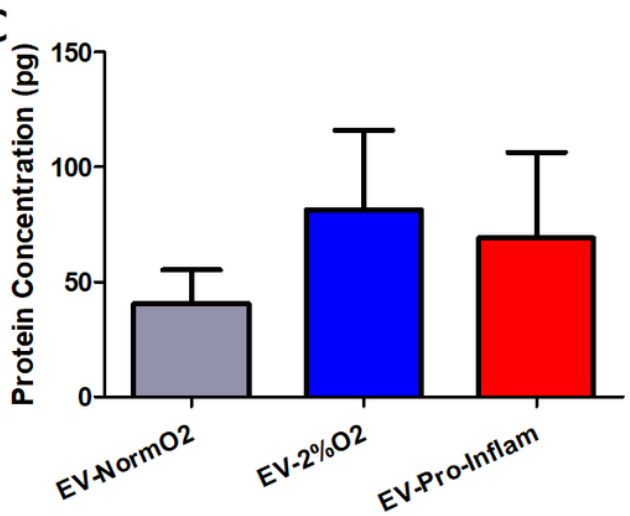

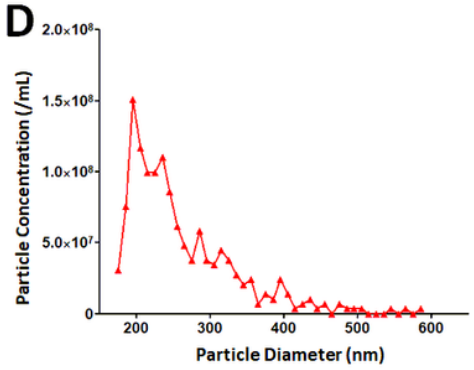

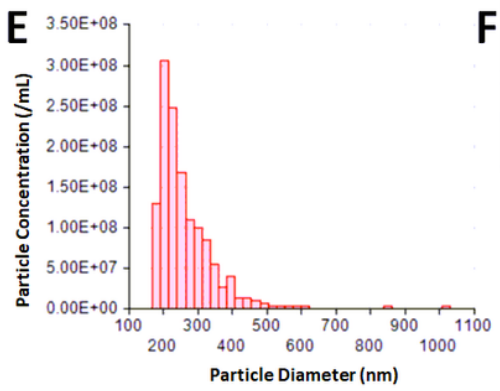

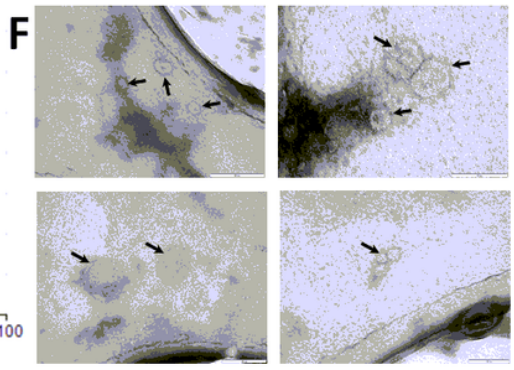

Figure 1

Detailed characterisation of EVs. (A) Representative flow cytometry analysis of EV-NormO2 preparations using MACSPlex exosome detection kit (Miltenyi) for the detection of CD9 (mean 81.25±5.03); CD63 (mean 94.59±2.23); and CD81 (mean 79.41±9.07) with unstained control beads. (B) Western blotting demonstrates presence of Alix and absence of cytochrome C in EVs (C) BCA assay assessment of total protein concentration in EV preparations from normoxic (21%O2, n=11), hypoxic (2%O2, n=8) and pro-inflammatory pre-conditioned MSC cultures (n=9), expressed as pg/mL per 1.0 x 106 cells. (D) (E) Representative output from particle concentration and EV sizing Nanopore analysis (Izon) tuned in the region ~80-300nm, highlighting EVs diameter range, with peak diameter averaging around 200nm with maximal diameter around 500nm (n=11) (F) TEM characterisation of hBM-MSC derived small EVs. Small EVs were re-suspended in sterile distilled water after isolation and spotted onto TEM grids before being stained with uranyl acetate. Black arrows indicate recorded small EVs. Small EVs were isolated from conditioned media taken from hBM-MSCs isolated from bone marrow aspirate cultured in hypoxic conditions (EV-2%O2).

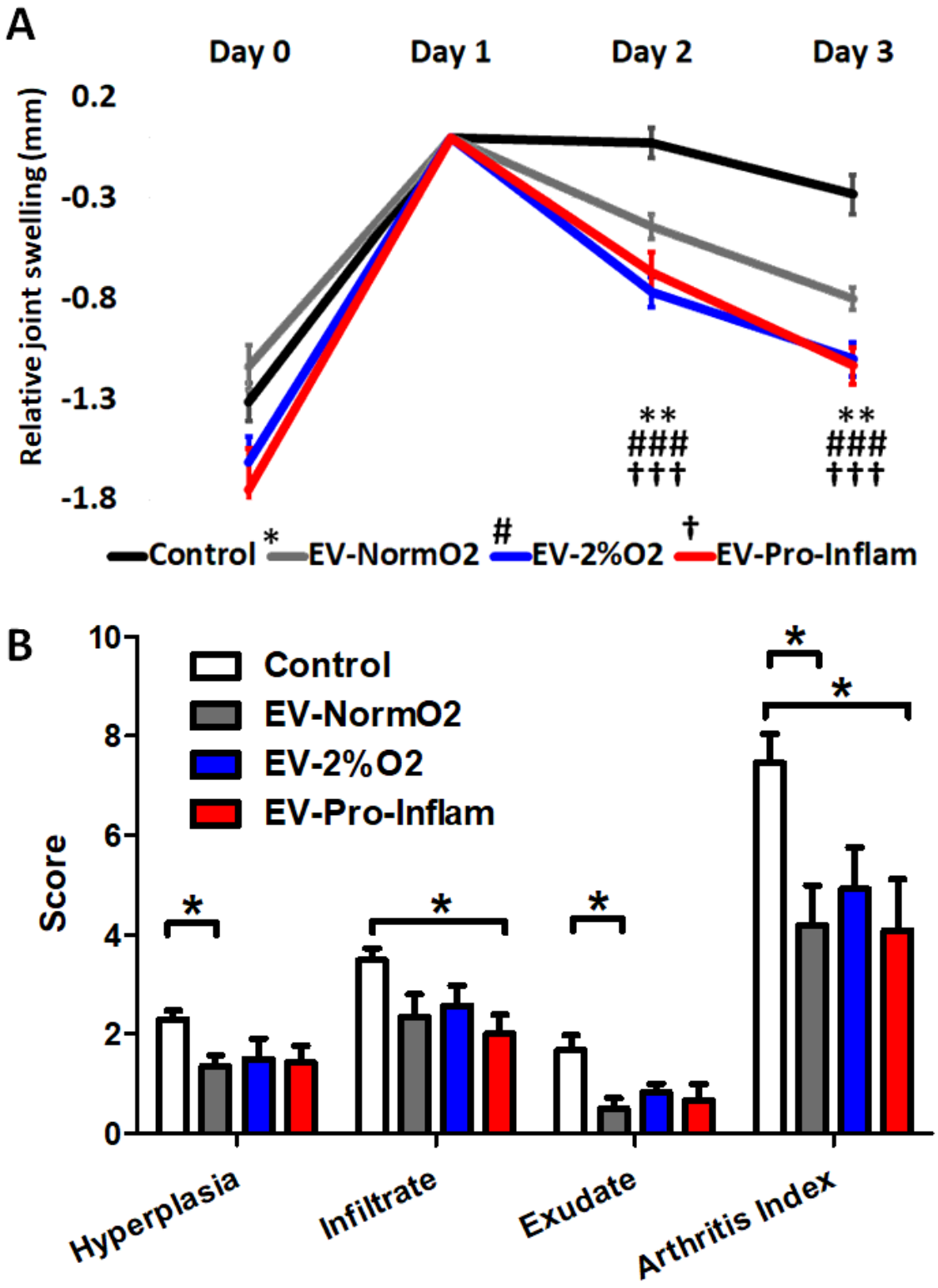

Figure 2

MSC-derived EVs treatment of mice with AIA. (A) Alleviation of joint swelling as a measure of therapeutic efficacy following EV treatments shows a significant effect of EVs compared to vehicle controls at day 2 and day 3 after arthritis induction; normalised to 0 at peak swelling (day 1). (B) Examination of histological signs of arthritis pathogenesis following EV treatment shows significant therapeutic effects of EVs sourced from MSCs cultured under normoxia and MSCs cultured in the presence of pro-

inflammatory cytokines. (Control n=21, EV-NormO2 n=8, EV-2%O2 n=6, EV-Pro-Inflam n=6); *p<0.05, **p<0.01, ***p<0.001.

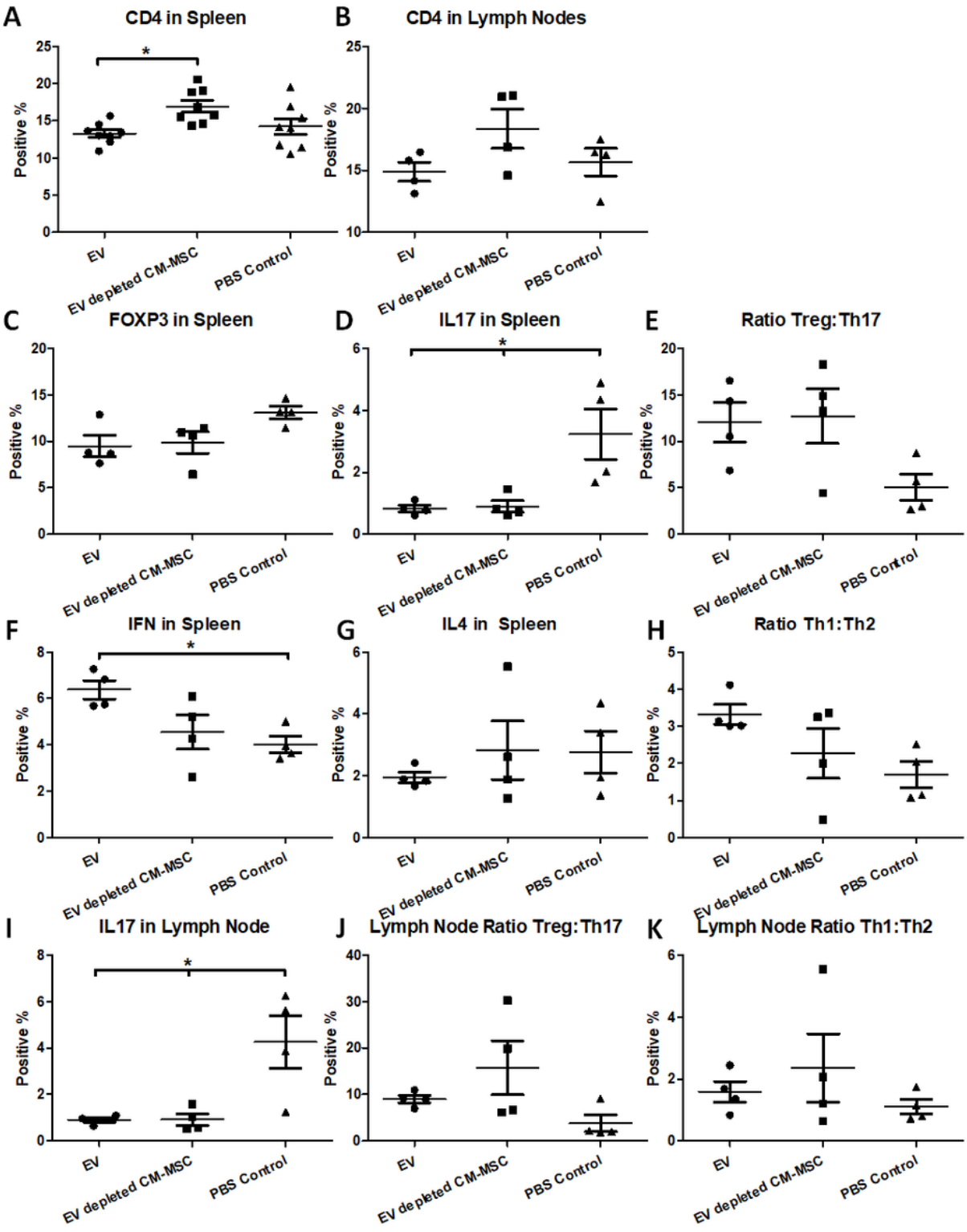

Figure 3

Outcomes of intracellular staining for T cell polarisation analysis. Intracellular staining for FACS analysis of IFN-γ, IL4 and IL17a in CD4+ T cells from EV-NormO2, EV-depleted CM-MSC or PBS control, showed

significant reductions in IL17a expression suggestive of reduced Th17 polarisation and a restoration of the Treg:Th17 balance in EV-NormO2 treated mice (n=4, *p<0.05).

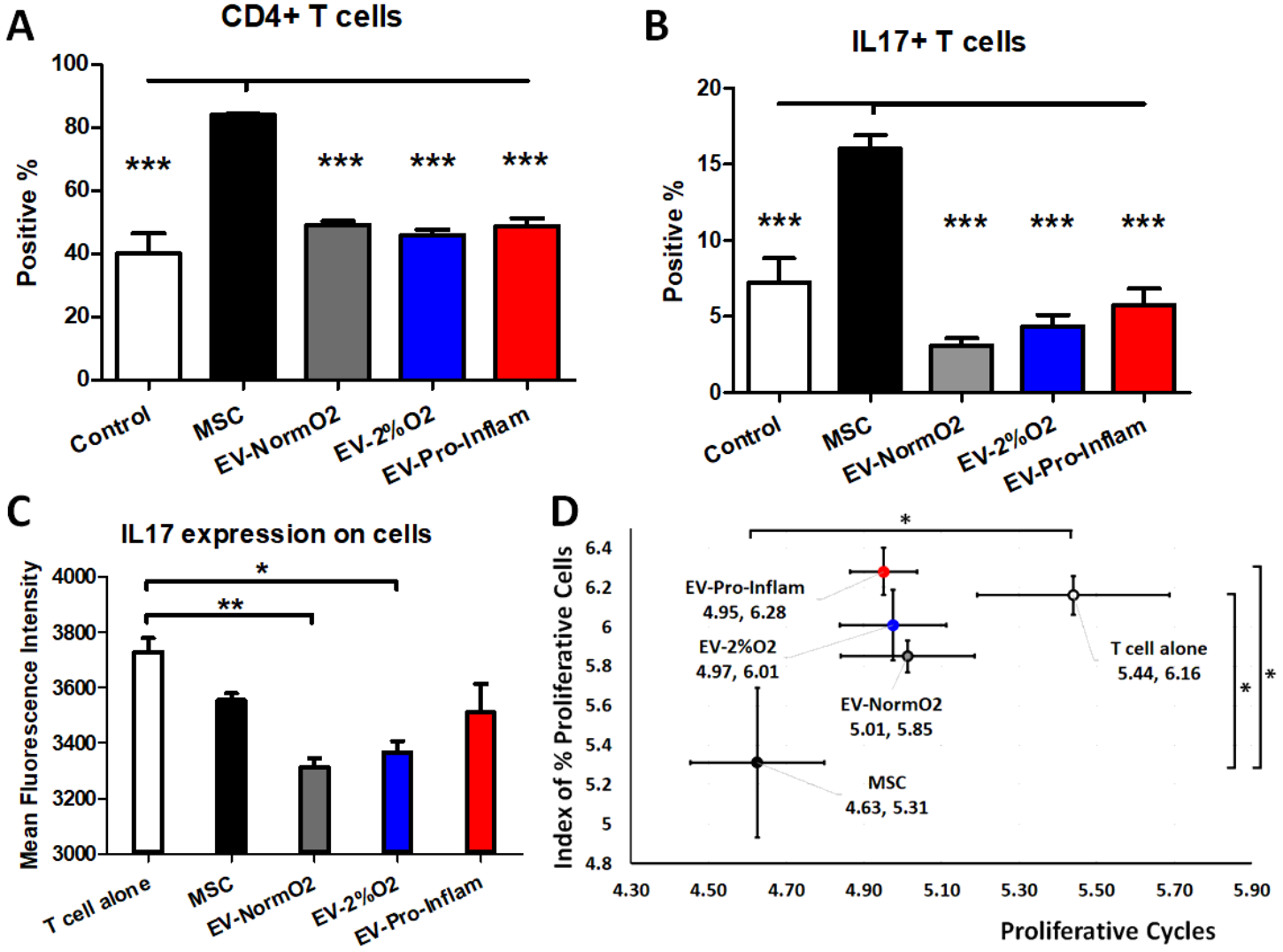

Figure 4

Outcomes of EV treatments co-cultured with T cells isolated from healthy murine spleens (A) Increased CD4+ Tcells in MSC co-cultures compared to EV-NormO2; EV-2%O2; EV-Pro-Inflam; and T cells alone control (n=3; ***p<0.001) (B) Increased pro-inflammatory Th17 cells (IL17a+) in MSC co-cultures over to EV-NormO2; EV-2%O2; EV-Pro-Inflam; and T cells alone control (n=3; ***p<0.001) (C) reduced expression of IL17a in CD4+IL17a+ T cells in EV-NormO2 and EV-2%O2 co-cultures (n=3; *p<0.05; **p<0.01) (D) MSC co-cultures significantly inhibited T cell proliferation compared with T cells cultured alone (both measures) and EV-Pro-Inflam co-culture (Index of proliferation only) (n=3; *p<0.05).

Supplementary Files

This is a list of supplementary files associated with this preprint. Click to download.

- SupplementaryFigure1.tif